How to cite: *Angew. Chem. Int. Ed.* **2023**, *62*, e202308008
doi.org/10.1002/anie.202308008

Slippery Surfaces | Hot Paper

Nanostructure Explains the Behavior of Slippery Covalently Attached Liquid Surfaces

*Isaac J. Gresham, Seamus G. Lilley, Andrew R. J. Nelson, Kaloian Koynov, and Chiara Neto**

Abstract: Slippery covalently-attached liquid surfaces (SCALS) with low contact angle hysteresis (CAH, $<5°$) and nanoscale thickness display impressive anti-adhesive properties, similar to lubricant-infused surfaces. Their efficacy is generally attributed to the liquid-like mobility of the constituent tethered chains. However, the precise physico-chemical properties that facilitate this mobility are unknown, hindering rational design.

This work quantifies the chain length, grafting density, and microviscosity of a range of polydimethylsiloxane (PDMS) SCALS, elucidating the nanostructure responsible for their properties. Three prominent methods are used to produce SCALS, with characterization carried out via single-molecule force measurements, neutron reflectometry, and fluorescence correlation spectroscopy. CO_2 snow-jet cleaning was also shown to reduce the CAH of SCALS via a modification of their grafting density. SCALS behavior can be predicted by reduced grafting density, Σ, with the lowest water CAH achieved at $\Sigma \approx 2$. This study provides the first direct examination of SCALS grafting density, chain length, and microviscosity and supports the hypothesis that SCALS properties stem from a balance of layer uniformity and mobility.

Introduction

A droplet of water easily glides across the surface of a thick oil layer due to negligible interfacial friction and the absence of defects. This frictionless scenario can be replicated on solid surfaces by trapping an infused interfacial layer of air (as in superhydrophobic surfaces),[1] or of oil (as in lubricant-infused surfaces)[2] using micro- and nano-textures. It is a recent discovery that even nano-thin oil layers, chemically grafted on solid smooth surfaces, can be just as slippery as oil-infused surfaces.[3] These new materials are named slippery covalently attached liquid surfaces (SCALS),[4] and can be thought of as a subset of the broad family of polymer brushes.[5,6] SCALS are typically composed of polydimethylsiloxane (PDMS), and their key distinguishing features are their exceptionally low values of contact angle hysteresis (CAH $\leq 5°$) with a wide range of liquids (both good and bad solvents, i.e. liquids in which the layer is swollen or collapsed, respectively), and the fact that the grafted nano-thin lubricant is not depleted over time.

The extremely low values of CAH in SCALS have been found to correlate with many desirable surface properties, such as easy droplet shedding, anti-fouling, anti-scaling, and lubrication, and interesting interfacial dynamics.[4,7–9] Having access to robust anti-adhesive surfaces could have broad technological and environmental benefits, for example by reducing hydrodynamic drag due to fouling, and increasing the efficiency of condensation processes. However, the structural and dynamical properties that differentiate SCALS from conventional polymer brushes, particularly with regards to their CAH, remain elusive. Although it is widely accepted that the liquid-like mobility of SCALS is responsible for their properties,[7,9] the specific molecular properties and timescales of dynamics important for this mobility are yet unknown.[4,10] Many reported PDMS SCALS have variable values of CAH (for water, between 1 and 15°), but the physicochemical reason for these vast differences is unknown. There are even arguments that SCALS are not a new material, but simply polymer brushes containing traces of monomers or ungrafted PDMS chains, which effectively works as an infused lubricant which can be depleted.[11]

The majority of SCALS preparation methods[3,12–14] do not control or characterize crucial structural properties such as grafting density (i.e. the average number of chains per unit area), chain length, and polydispersity (hereafter referred to collectively as *nanostructure*). The current structural information provided (chiefly layer thickness and roughness) is not sufficient to explain the low CAH of SCALS[4] or describe the link between their nanostructure and hypothesized 'liquid-like' mobility. The molecular weight of the grafted chains is generally unknown due to imprecise grafting techniques, unless specific grafting to approaches are used.[15–17] However, these

[*] Dr. I. J. Gresham, S. G. Lilley, Prof. C. Neto
School of Chemistry and the University of Sydney Nano Institute, The University of Sydney, Sydney, NSW, Australia
E-mail: chiara.neto@sydney.edu.au
Dr. K. Koynov
Max Planck Institute for Polymer Research, Mainz, Germany
Dr. A. R. J. Nelson
Australian Center for Neutron Scattering, ANSTO, Sydney, NSW, Australia

precise grafting to methods do not necessarily produce low adhesion surfaces with minimum CAH, and they do not independently control grafting density, which limits their ability to explore the full range of possible SCALS structures.[15–17] The chain length, grafting density, and polydispersity of SCALS have never been directly measured, and in many cases cannot even be sensibly approximated.

From a chemical perspective, SCALS bear many similarities to 'polymer brushes', which have attracted much attention over the past decades.[6] In polymer brush theory, the system behavior scales with the (dimensionless) reduced grafting density Σ, which indicates the degree of chain stretching.[18] Below $\Sigma = 1$, the layer is in the mushroom regime, otherwise it is in the brush regime. Reduced grafting density is calculated via:

$$\Sigma = \sigma \pi R_g^2 \tag{1}$$

Where R_g is the average radius of gyration of grafted polymers and σ is the grafting density. R_g is dependent on the solvent condition that the polymers are in; as our probe liquid (water) is a non-solvent for PDMS, R_g can be calculated from the radius of a sphere with the same volume as the grafted PDMS chain (see SI, section 8.1). σ is calculated here via:

$$\sigma = \frac{\rho d_{dry}}{\hat{N}_n M_m} \tag{2}$$

Where ρ is the polymer density, d_{dry} is the dry thickness of the polymer layer,[19] $\hat{N}_n$ is the (number average) degree of polymerization, and M_m is the molecular weight of the repeat unit (74.15 $g\,mol^{-1}$ for PDMS). The polydispersity of tethered chains can influence the behavior of the layer, and is characterized by the polydispersity index, PDI, i.e. the ratio of the number average to weight average molecular weight.

In this work several literature methods for the synthesis of PDMS SCALS are reproduced, and their thickness, roughness and CAH are compared to literature values. The combination of atomic force microscopy single-molecule force measurements (AFM-SMFM) and neutron reflectometry (NR) allows us to directly measure $\hat{N}_n$ and σ. The conclusion is that the water CAH of PDMS SCALS can be satisfactorily predicted by the reduced grafting density of the layers for the SCALS studied here, with a minimum existing around $\Sigma = 2$. These conditions correspond to a minimum in layer microviscosity, as shown using fluorescence correlation spectroscopy (FCS).

Results and Discussion

Preparation of SCALS and initial characterization

Three prominent methods for the preparation of SCALS were selected from the literature and reproduced in our laboratories, with thorough cleaning procedures. There are many more methods for producing PDMS SCALS (and indeed, SCALS with different chemistries), each with their own advantages; this work is comprehensively summarized in our recent review.[4] Full details of the synthetic methods used are available in SI, while a summary of key parameters and naming conventions for samples is given in Table 1. Briefly, the three chosen methods are those of:

- Krumpfer and McCarthy (K)[3] (Figure 1a); the simplest method, in which methyl-terminated silicon oil of different viscosity (higher viscosity corresponds to higher $\hat{N}_n$) is spread over a silicon wafer (covered in native silicon oxide, Si/SiOx) and heated to 100 °C for 24 h. The PDMS spontaneously splits along its backbone in one or more locations (catalyzed by the presence of water)[20] and PDMS chains of unknown length react with surface silanol groups. Because of its simplicity, ubiquity,[11,21,22] and ease of varying the precursor $\hat{N}_n$, this method is used to prepare a series of SCALS here.
- Wang and McCarthy (W)[12] (Figure 1b); a popular and rapid method in which Si/SiOx wafers are coated with a solution of dimethoxydimethylsilane (a PDMS monomer) and sulfuric acid in isopropyl alcohol. As the alcohol evaporates, the increasing concentration of the silane and acid result in a polycondensation reaction which produces grafted-from brushes of end-tethered PDMS.
- Zhang et al. (Z)[13] (Figure 1c); in this recent method chlorine-terminated PDMS polymers are deposited from the vapor phase onto Si/SiOx wafers. Zhang et al. claim that these polymers undergo a polycondensation reaction, producing exceptionally thick (30 nm) layers. While we could not reproduce this layer thickness, our subsequent characterization confirms that this polycondensation reaction mechanism occurs.

Table 1: Synthetic details for each of the SCALS studied in this work. Materials and methods can be found in Section 1 and 2 of the Supporting Information.

Sample	Method	Reagent	*N*	Reaction conditions
W1	[12]*	$Me_2(MeO)_2Si$	1	1 min, 25 °C, 1 bar
W2	[12]*	$Me_2(MeO)_2Si$	1	20 min, 25 °C, 1 bar
K1	[3]	20 cSt Me-PDMS-Me	≈25	24 h, 100 °C, 1 bar
K2	[3]	50 cSt Me-PDMS-Me	≈50	24 h, 100 °C, 1 bar
K3	[3]	200 cSt Me-PDMS-Me	≈125	24 h, 100 °C, 1 bar
K4	[3]	350 cSt Me-PDMS-Me	≈190	24 h, 100 °C, 1 bar
K5	[3]	10 kcSt Me-PDMS-Me	≈750	24 h, 100 °C, 1 bar
Z1	[13]	Cl-PDMS-Cl	≈40	60 min, 60 °C, 5 mbar

* Method was adapted from literature to enable large uniform coating area for NR, see corresponding methods section in Supporting Information.

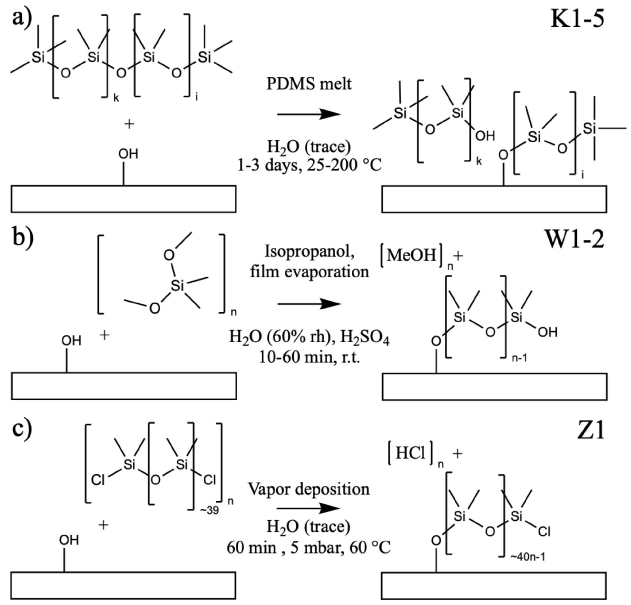

Figure 1. Reactions Schemes used to prepare the SCALS in the current work. a) The spontaneous grafting of neat silicon oil first documented by Krumpfer and McCarthy,[3] b) the methoxysilane condensation polymerization approach of Wang and McCarthy,[12] c) the vapor-phase polycondensation of chlorine-terminated PDMS oligomers documented by Zhang et al.[13] Details of synthetic methods are provided in Section 2 of the Supporting Information. Reprinted from Advances in Colloid and Interface Science vol. 315, I. J. Gresham and C. Neto, "Advances and challenges in slippery covalently-attached liquid surfaces", p. 102911, Copyright 2023, with Permission from Elsevier.[4]

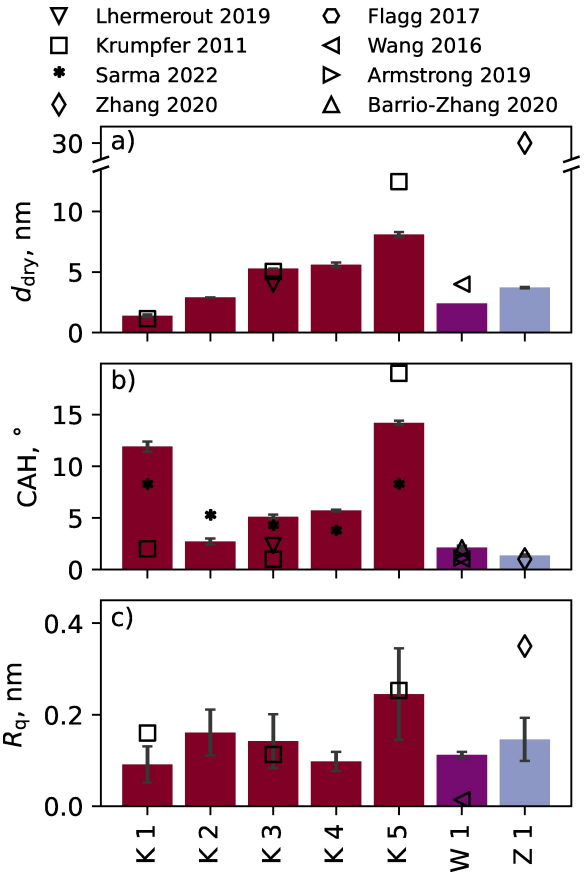

Figure 2. Comparison of the a) layer thickness, b) contact angle hysteresis (CAH), and c) RMS surface roughness of the SCALS prepared in this work (bars) compared to respective literature values (symbols). Error bars correspond to one standard deviation, on at least 5 measurements of CAH and thickness. The values of thickness and CAH for the SCALS prepared by us match those reported in the literature, except for the work of Zhang et al. References and synthetic details are given in Table 1. Other references identified in the legend are [3, 13, 21–24].

All methods result in an end-tethered linear polymer brush in either a loop or dangling-chain configuration. Loops and dangling chains were not distinguished in subsequent characterization. The key assumption made is that a loop with molecular weight x is equivalent to two dangling ends with molecular weight $x/2$. The effect of the number of grafting points on the CAH of PDMS SCALS has been investigated by Flagg and McCarthy.[15] A discussion of this work can be found in Section 4 of the Supporting Information. Briefly, to determine the effect of polymer configuration on CAH, careful synthetic methods such as that of Flagg and McCarthy must be coupled with advanced characterization, such as that used in the present work.

The d_{dry}, CAH, and RMS roughness (R_q) of the prepared SCALS were measured via ellipsometry, sessile drop goniometry, and AFM, respectively, and are shown in Figure 2 (see Figure S3 and S4 for AFM images). These measurements were made before CO_2 snow jet cleaning (described in the following section) was performed. Our results are consistent with the values reported in the literature (with the exception of the Z1 thickness, discussed later), with small differences reconcilable by slight variations in the reagents used. As extensive washing steps were performed, our successful replication of such a wide range of PDMS SCALS confirms that the slipperiness of these layers is not due to residual unreacted PDMS.

The first observation is that in the Krumpfer SCALS (K1–K5 in Figure 2), the layer thickness increases as the PDMS precursor viscosity increases, and a CAH minimum (1.5°) is found when grafting PDMS of intermediate viscosity (50 cSt). Both of these trends (an increase in thickness with increasing viscosity and a CAH minimum at intermediate viscosities) match those reported elsewhere.[3,11,21,22] However, the viscosity of the precursor PDMS at which the CAH minimum is observed differs between studies, indicating that secondary factors such as the silica hydration state and polydispersity of the PDMS oil used contributes to the structure and performance of SCALS prepared via the Krumpfer method. In our results, both the thinnest layers (K1, 1.5 nm thick) and thickest layers (K5, 8 nm thick), had high CAH (12 and 15°, respectively), while the other layers classify as SCALS by our definition,[4,9] with CAH below 5°. Secondly, a pronounced difference in thickness between our surfaces and those reported by Zhang et al.[13] was found. While their reported CAH (<1.5°) was reproduced, the thickness

measured here (4 nm) was much lower than that reported (30 nm). Further investigation is needed to fully understand this discrepancy. Lastly, all the surfaces are ultra-smooth, with RMS roughness below 0.3 nm; within the range of subnanometer roughness measured, no correlation was observed between surface roughness R_q and CAH.

Effect of CO_2 snow-jet cleaning on CAH

In an attempt to reduce dust and other particulate defects, the substrates were cleaned using a CO_2 snowjet;[25] snow-jet cleaning is used for non-destructive removal of particulates and organic contaminants from hard substrates, e.g., in the automotive and semiconductor industries. AFM imaging confirmed that CO_2 cleaning removed particulate defects. More importantly, CO_2 snow jet cleaning modified the nanostructure of thicker SCALS. Modification of SCALS structure with snow-jet cleaning provides insight into the origin of SCALS behavior.

The thickness and water CAH of the Krumpfer SCALS are shown in Figure 3, before and after snow-jet cleaning. After snow-jet cleaning, the thicker PDMS coatings became

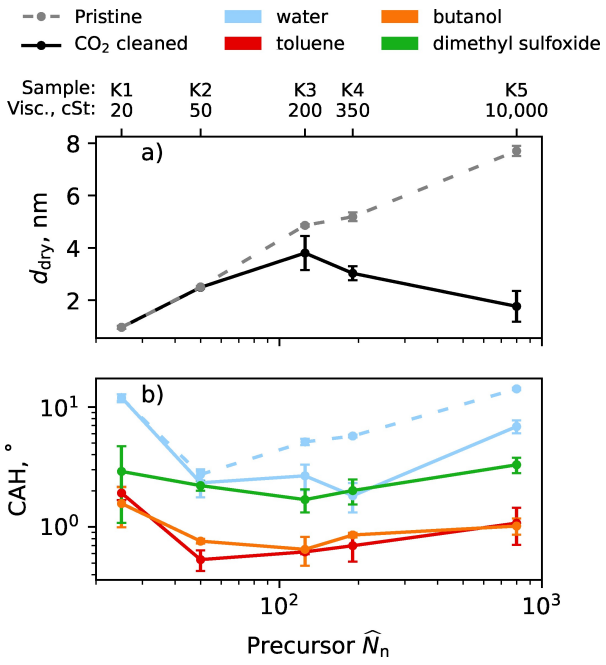

Figure 3. a) Ellipsometric thickness of SCALS prepared via the Krumpfer method, before (pristine) and after CO_2 snow jet cleaning. Cleaning reduced d_{dry} for samples prepared from higher viscosity PDMS (K3–K5), but had no observable effect on lower viscosity samples (K1–K2). d_{dry} measurements are averaged across three identically-prepared wafers (five points per wafer). b) CAH for a range of solvents; measurements are averaged across three identically-prepared wafers (four points per wafer). Error bars correspond to one standard deviation. Water CAH were measured before (dashed) and after (solid line) CO_2 snow-jet cleaning; water CAH reduced for K3–K5 after CO_2 cleaning, but K1–K2 were within error. All other solvents were measured after CO_2 cleaning, and also exhibited a CAH minimum at intermediate viscosity.

significantly thinner, by 2 to 6 nm. For the same surfaces, their CAH decreased dramatically, by 5 to 10°. These treated surfaces retained low CAH for a wide range of solvents (CAH of toluene, butanol, and dimethyl sulfoxide are shown in Figure 3). Interestingly, the Krumpfer SCALS exhibited a minimum CAH at intermediate viscosity of about 50 to 200 cSt (i.e. intermediate molecular weight) for all liquids tested. This indicates that the sample physical properties are responsible for the layer slipperiness in good and bad solvents.

Based on the thickness decrease, CO_2 snow-jet cleaning removed strongly-adsorbed PDMS from surfaces K3–K5, i.e. the SCALS with higher thickness and higher $\hat{N}_n$, but the CAH did not increase, rather it decreased. This is not simply due to the removal of particulate contaminants or ungrafted PDMS, as these would also be present on K2, which is not significantly affected by cleaning; rather, it must be due to a change in the structure of the layer. It has been observed before that different surfaces exhibit different durability.[4] Our results indicate that the structure of SCALS with longer chain lengths is more easily damaged than that of SCALS with shorter chain lengths; the same observation was made by Monga et al.[26] when different chain lengths layers were exposed to steam condensation conditions. It is likely that long chains are mechanically removed by the high-velocity fluid present during CO_2 cleaning. Hydration and steric forces are known to facilitate the cleaving of tethered polymers at the grafting point;[27,28] a similar effect is expected from the applied shear force during CO_2 cleaning. The stress at the grafting point is expected to increase with the number of monomers in the chain, which explains why longer chains are damaged by CO_2 cleaning.

Figure 3 also highlights the shortcomings of the present extent of SCALS characterization. While it can be reasoned that higher viscosity oils produce layers with higher $\hat{N}_n$, this has not been confirmed. Similarly, while it is reasonable that snow-jet cleaning changes the structure of the SCALS, it is not known whether it affects $\hat{N}_n$, σ, PDI, or a combination thereof.

Characterization of SCALS Nanostructure

Two techniques, AFM single molecule force measurements (AFM-SMFM) and neutron reflectometry (NR), were used to characterize degree of polymerization $\hat{N}_n$, grafting density σ, and PDI of the prepared SCALS. Together with the CAH characterization in Figure 2, this allowed layer performance to be linked to structure.

NR measures the intensity of a neutron beam reflected from the interface of interest as a function of the scattering vector, Q (e.g., Figure 4a). NR datasets are available on Zenodo.[29] From this NR signal, the surface-normal density profile of the interface averaged over several cm^2 (Figure 4b) can be extracted through a model-optimization process; here a previously documented freeform approach was used with no a priori assumptions regarding layer structure.[19] To interpret the derived profiles and extract information regarding $\hat{N}_n$ and PDI, numerical self-consistent

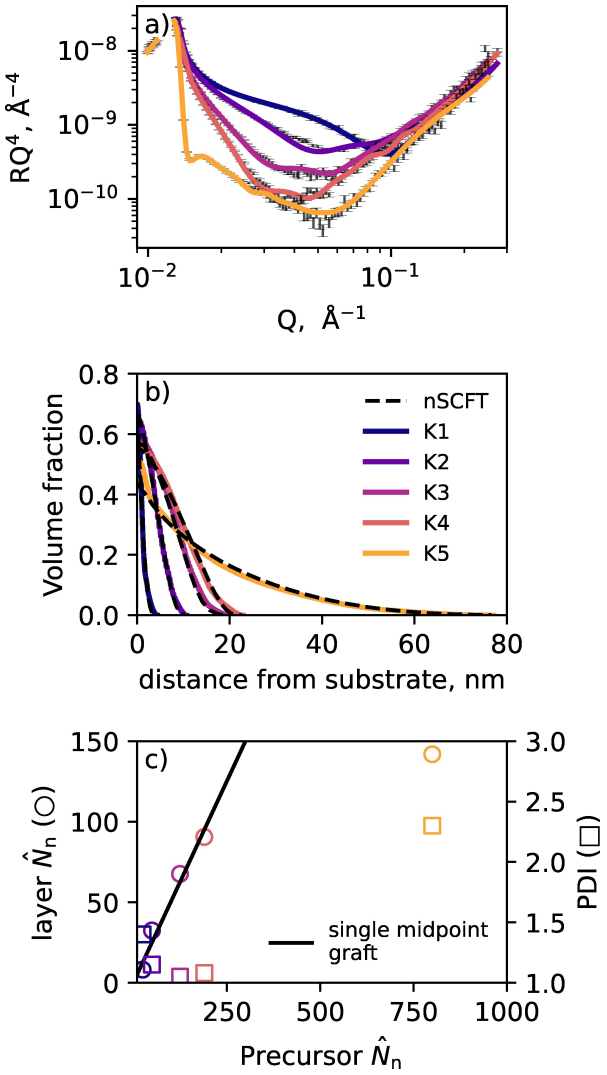

Figure 4. a) Neutron reflectometry data (black error bars) and corresponding model fits (colored lines) for PDMS layers prepared according to the Krumpfer method, samples K1–K5, in deuterated toluene, plotted as RQ^4 vs log(Q). b) PDMS volume fraction profiles for samples K1–K5 that correspond to the modeled reflectometry profiles in (a), along with profiles generated by nSCFT (black dashed lines). c) Degree of polymerization in the layer $\hat{N}_n$ and polydispersity PDI, extracted from the nSCFT in (b), as a function of approximate $\hat{N}_n$ of the precursor oil. The legend in b) refers to all parts of the Figure.

field theory (nSCFT)[30,31,32,33] was used. For a given molecular weight distribution, nSCFT produces a volume fraction profile, which can be directly compared to NR output. Here, the PDMS molecular weight distribution is described by the Schulz-Zimm distribution—a standard method for describing polymer polydispersity that takes $\hat{N}_n$ and PDI as fitting parameters (see Table S1 for details). By tuning the nSCFT inputs such that its output matches that of the freeform method, $\hat{N}_n$ and PDI could be extracted. All NR data collected are included in Figure S5 to S12, alongside fitted model-free and nSCFT profiles.

AFM-SMFM measures the force acting on an AFM tip as it withdrawn from a surface coated with grafted polymers, allowing for the length of chains physisorbed to the tip to be measured through observation of individual detachment events. AFM-SMFM are ideally suited to measure directly chain length.[34,35] However, any point in the chains may be picked up and the results obtained tend to be biased toward longer chains which are more likely to reside at the top of the layer. A representative single molecule force measurement is shown in Figure 5a. Chain length can be directly transformed to N by dividing by the monomer length (0.32 nm for PDMS), and information on polydispersity (PDI) can be derived by taking many hundreds of measurements. Representative N distributions are shown in Figure 5b, 5c, while all N distributions are included in Figure S13. Individual force curves and fits for a single experiment are shown in Figure S1. Further examples are provided in the SI; complete datasets and videos of analysis are available on Zenodo,[29] while code is available on GitHub.[36]

These two techniques complement each other, as NR-nSCFT is sensitive to all chain lengths but provides an indirect measurement of length, while AFM-SMFM directly

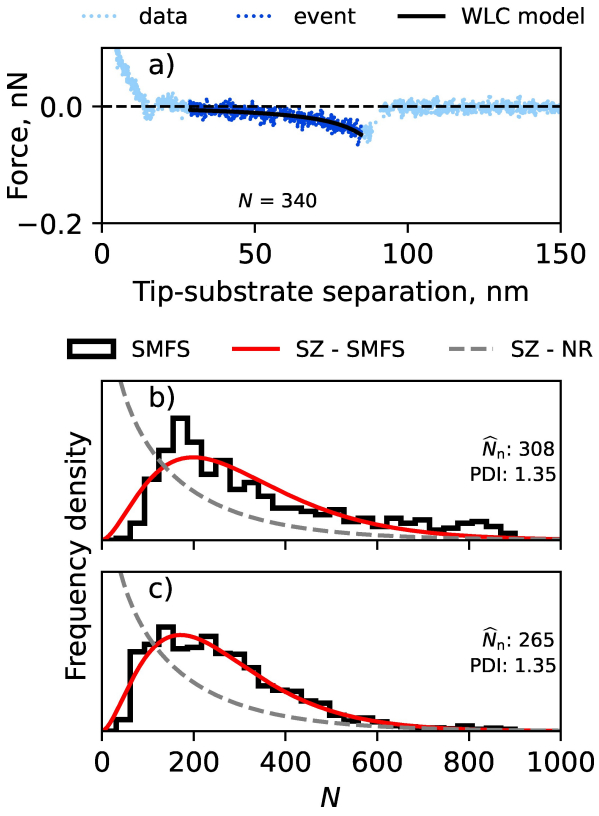

Figure 5. a) A representative force curve showing a single-molecule event selected by our algorithm (dark blue) as well as the fitted worm-like chain model (black). The number of repeat units for the fit is 340. b, c) Frequency density histograms (black lines) derived from AFM-SMFM for sample K5 b) before and c) after CO_2 snow jet cleaning. Red lines are from a Schulz-Zimm distribution which was fitted to the collected histogram to derive $\hat{N}_n$. Grey lines are from the Schulz-Zimm distribution derived from NR-nSCFT in Figure 4 for K5 prior to snow-jet cleaning; while both techniques predict similar maximum chain length ($N \approx 800$), NRnSCFT is more sensitive to the presence of short chains.

measures chain length but is only sensitive to long chains. Two case studies are used to demonstrate the power of these techniques and answer pertinent questions: First, NR-nSCFT was used to understand the widely used Krumpfer reaction.[3,11,20–22] Second, AFM-SMFM was used to measure the effect of CO_2 snow-jet cleaning on the nanostructure of thicker SCALS.

Understanding the Krumpfer reaction

The NR data revealed the relationship between the degree of polymerization $\hat{N}_n$ in the precursor oil and that in the grafted layer for the Krumpfer reaction (Figure 1a). The colored lines in Figure 4b show the surface-normal volume fraction profiles for samples K1–K5 using the 'model-free' analysis mentioned above.[19] These profiles were matched almost exactly by nSCFT, with $\hat{N}_n$ and PDI being varied to optimize the agreement between the two profiles; fitted parameters are given in Figure 4c. There is a clear correlation of the precursor $\hat{N}_n$, extracted from the PDMS viscosity, with the $\hat{N}_n$ of the grafted layer. If each chain broke exactly once (see reaction Scheme in Figure 1a) at its midpoint (on average), the trend shown by the black line in Figure 4c would be expected. At low precursor $\hat{N}_n$, the measured values match this singlebreak model almost exactly, while at higher precursor $\hat{N}_n$ the values deviate from it; the PDI increases with precursor $\hat{N}_n$. This result is explained by the fact that at low $\hat{N}_n$, precursor PDMS chains react only once, while at higher $\hat{N}_n$, precursor PDMS chains reacts multiple times, consistently with the hypothesized reaction mechanism.[20] This result demonstrates that the molecular weight of the grafted chains can not be approximated by the viscosity of the PDMS melt used for the functionalisation, contrary to what has been done in the literature.[22,21]

Structure before and after CO_2 snow-jet cleaning

The effect of CO_2 snow-jet cleaning on the structure of the K5 grafted layers was studied by the AFM-SMFM technique and the results compared to the NR-nSCFT study. Out of approximately 6000 force curves (for each surface), over 500 were identified as containing single-molecule events, which were extracted and analyzed using a Rouse-type model. Approximately one in ten approach-retract cycles resulted in the attachment and subsequent stretching of one or more single molecules. A demonstration of this approach is provided in Figure 5a, and all force curves and fits are in SI. Force measurements were performed before and after snow-jet cleaning, with the resulting chain length plotted as a frequency density histogram in Figure 5b, 5c. The $\hat{N}_n$ and PDI were extracted by fitting these histograms with a Schulz-Zimm distribution, which enabled comparison with the NR-nSCFT data.

As shown in Figure 5, CO_2 snow-jet cleaning had a negligible effect on $\hat{N}_n$, which decreased only by 14 % (308 to 265; the PDI was unchanged). On the other hand the layer thickness decreased by 75 % upon CO_2 snow-jet cleaning (Figure 3). Therefore, it appears that CO_2 snow-jet cleaning primarily decreased SCALS thickness by reducing the grafting density. Long chains at high grafting densities are likely to experience a higher tension on siloxane bonds close to or at the grafting site. As grafting density is decreased, the chains can lie flat on the surface, allowing mechanical force to be transferred to the substrate, rather than the grafting point, preventing further degrafting. As the grafting density decreased, shorter chains became more accessible to the AFM tip, explaining the slight shift in the Nn distribution to shorter chains upon snow-jet cleaning.

The shortcomings of AFM-SMFM can be seen by a comparison with the Schulz Zimm distribution derived from NR, which is shown as a grey dashed line in Figure 5b, 5c. The length of the tail region predicted by NR-nSCFT and AFM-SMFM are similar, with both measuring no chains above approximately $\hat{N} = 800$. However, NR-nSCFT indicates the presence of a large number of short chains, which reside close to the substrate. The presence of these short chains is congruent with the expected reaction mechanism (Figure 1a, Figure 4). It is likely these chains are not picked up by AFM-SMFM, as they are prevented from physisorbing to the AFM tip by longer chains, which reside at the the top of the SCALS.

Correlating CAH with nanostructure

Using the techniques explained above, CAH can be linked to surface nanostructure, as shown in Figure 6. As most of the samples were prepared via the Krumpfer method, $\hat{N}_n$, d, σ are expected to be covariant, as $\sigma \propto \hat{N}_n^{-1}$ for brushes prepared via grafting-to. Below, each parameter is discussed in turn. Generally, values measured by the NR-nSCFT method are more accurate than those attained via SMFM; hence, where values are reported, they are taken from NR-nSCFT.

- *Chain length* (a, d): If snow-jet cleaned samples are ignored, a minimum in CAH is observed at intermediate $\hat{N}_n$ by both NR and AFM-SMFS (40 and 80 repeat units, respectively) consistent with previous studies.[3,11,15,21] Snow-jet cleaned samples (i.e., K5), which have similar chain lengths but different grafting densities, break this trend, indicating that SCALS cannot be described by $\hat{N}_n$ alone.
- *Thickness* (b, e): Consistent with trends in the existing literature,[4] Figure 6 shows a CAH minimum at intermediate layer thickness (between 2 and 5 nm) as measured by both NR and ellipsometry. This trend with thickness is present even across snow-jet cleaned samples.
- *Grafting density*: No consistent trend was observed between σ and CAH; data is plotted in Figure S14.
- *Reduced grafting density* (c, f): All samples studied here exhibit a minimum CAH at either $\Sigma = 2$ (AFM-SMFM) or $\Sigma = 2.5$ (NR-nSCFT).

The lowest hysteresis samples studied here (K2, W1, Z1) all possessed similar nanostructure, with $\hat{N}_n \approx 40$ (≈ 3 kDa)

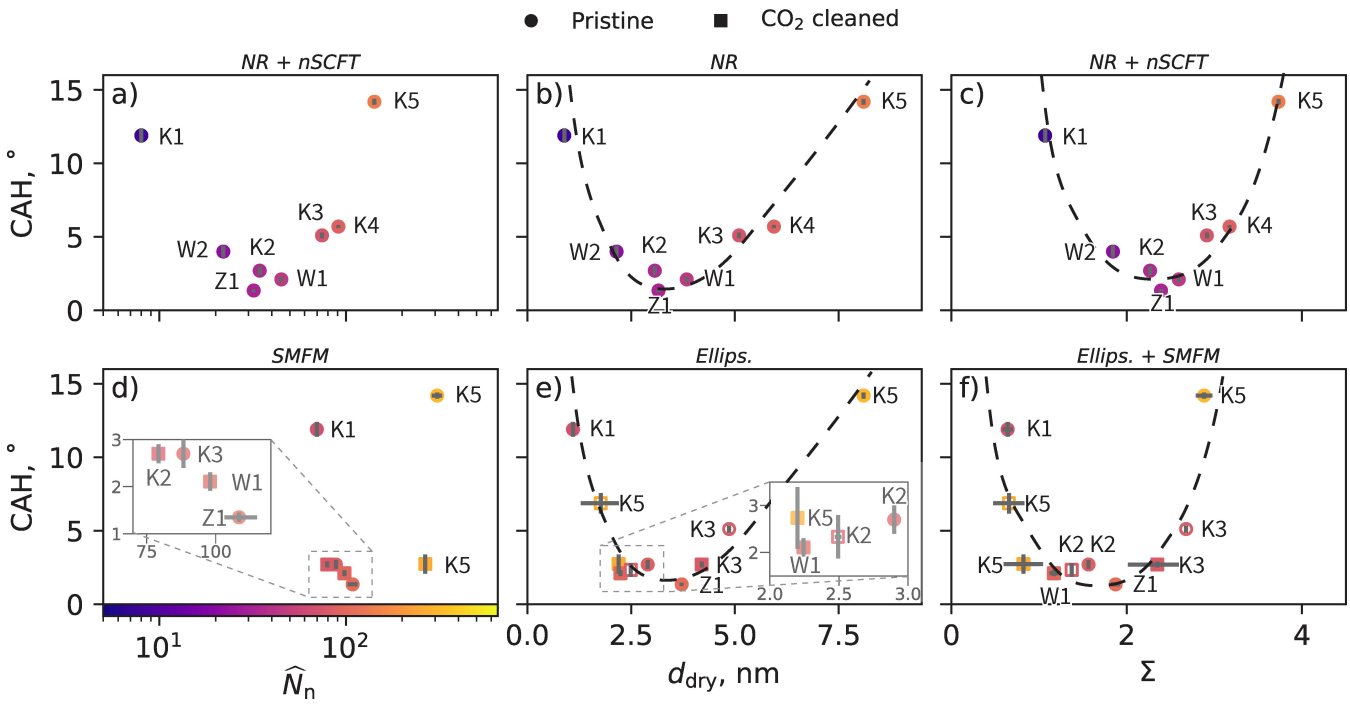

Figure 6. Contact angle hysteresis (CAH) as a function of nanostructural parameters as measured by (ac) NR + nSCFT and (d–f) AFM-SMFM/Ellipsometry: a, d) $\hat{N}_n$ number of repeat units in the grafted chains (coded by color temperature on subsequent plots), b, e) d_{dry} layer thickness, c, f) Σ reduced grafting density. Pristine samples are marked with circles, CO_2 cleaned samples are marked with squares; each data point is marked with the synthetic method used to prepare it (see Table 1). Hollow markers in parts e) and f) correspond to the thickness and water CAH data from Figure 2, with chain length approximated by assuming no change in $\hat{N}_n$ with CO_2 cleaning (based on Figure 5). They are included here to better establish trends.

and $d_{dry} \approx 3.5$ nm (corresponding to $\Sigma = 2.5$). Previous work has speculated that a minimum in CAH is observed for polymers of intermediate molecular weight as shorter chains imperfectly coat the substrate, and longer chains are above the bulk entanglement length of PDMS,[4,11,22,26,37] which is between 6 and 34 kDa ($\hat{N}_n = 81$ to 460).[38,39] However, our study reveals that the exact value of entanglement length in the bulk is not significant, as entanglement is a function of σ for polymer brushes.[40] Consequently, arguments that rely solely on $\hat{N}_n$ and bulk entanglement length to explain SCALS behavior are incomplete.

As discussed above, CO_2 snow-jet cleaning results in a reduction in σ, but no appreciable change in $\hat{N}_n$. Hence, comparison of cleaned and pristine samples allow for the study of the effect of changing σ at constant $\hat{N}_n$; this revealed that the measured values of CAH cannot be explained independently by either parameter. Only the dimensionless reduced grafting density, Σ (Eq. (1)), which accounts for both σ and $\hat{N}_n$, is a predictor of SCALS performance. An examination of the literature where a calculation of Σ is possible[15] reveals the same trend and excellent agreement with our NR data (Figure S2c).

Classical polymer brush literature identifies Σ as one of the key parameters governing brush properties. However, this concept has not been central to contemporary understanding of SCALS behaviour. Recently, Σ has been reinvented and applied to a PEO SCALS system by Vahabi et al.,[41] who term it the "nondimensional slipperiness factor". Our recent neutron reflectometry characterization of these PEO SCALS found their structure to be consistent with that of true monolayers (i.e., no silane cross-linking).[42] That reduced grafting density can explain the CAH of both PEO and PDMS SCALS is further evidence that their slipperiness is due to similar mechanisms.

Interestingly, thickness remains an excellent predictor for CAH, even when σ and $\hat{N}_n$ are changed. By rearranging Eqs. (1) and (2), it can be shown that:

$$\Sigma = k\sigma\left(\frac{\hat{N}_n M_m}{\rho}\right)^{2/3},\ d_{dry} = \frac{\hat{N}_n M_m \sigma}{\rho} \tag{3}$$

where k is a constant equal to $\pi(\frac{3}{4\pi N_A})^{2/3}$; a full derivation is supplied in SI. Hence, d_{dry} and Σ exhibit identical scaling as σ is varied, and similar scaling with $\hat{N}_n$ ($\Sigma \propto \hat{N}_n^{2/3}$, $d_{dry} \propto \hat{N}_n$). This offers a potential explanation for the apparent dependence of CAH on layer thickness. Layer thickness could be an indirect measure of mobility (via Σ), rather than directly influencing CAH.

As noted above, the method outlined by Zhang et al.[13] produced a layer thickness much lower than the one reported in their work (4 nm vs. 30 nm). However, the AFM-SMFM characterization of $\hat{N}_n$ indicated that the polycondensation of chlorine-terminated oligomers (Figure 1c, used to explain the high thickness) is indeed occurring during this synthesis. Perhaps fine tuning of

reaction parameters (e.g., the partial pressure of H_2O within the vacuum chamber or hydration of the substrate) is required to produce thick layers. The existence of such thick SCALS challenge the trends observed within this work and throughout the literature.[4]

The evidence presented so far demonstrates that SCALS performance can be explained by the reduced grafting density, Σ. This finding is congruent with the explanation that both layer uniformity and mobility underpin the SCALS phenomenon. In order to achieve optimal SCALS, grafted chains must appropriately cover the substrate with a dense brush ($\Sigma > 1$), be long enough to be mobile ($\hat{N}_n > 20$), but not be so tightly-packed that the mobility is lost through entanglement ($\Sigma < 3$). The existence of a minimum chain length required for SCALS behavior is supported by combining our results with those of Flagg and McCarthy[15] (Figure S2). This link between mobility and structure was investigated by probing the microviscosity of the SCALS through fluorescence correlation spectroscopy (FCS).

Relationship between structure and layer microviscosity

Fluorescence correlation spectroscopy (FCS) measures the fluctuations of fluorescent light intensity caused by the diffusion of fluorescent tracers through a small observation volume ($<1\ \mu m^3$), typically formed by the focus of a confocal microscope. Correlation analysis of these fluctuations provides information on the diffusion time, τ_D, that the tracers need to cross the observation volume and thus on their diffusion coefficient and the mobility (viscosity) of the environment.[43] Here, FCS was used to study the diffusion of small (≈ 1 nm) terrylene diimide (TDI, inset in Figure 7) dye tracers, dispersed in PDMS SCALS covered by water. To this end SCALS corresponding to samples K1, K3, and K5 were prepared on glass coverslips. The TDI dye was dissolved in hexane and a droplet of this solution placed onto the PDMS SCALS. The hexane was allowed to evaporate, leaving TDI adsorbed within the SCALS layer. K1 and K5, which are considered non-slippery grafted layers, were grafted with the lowest ($\hat{N}_n$, precursor ≈ 15, $\hat{N}_n \approx 8$) and highest ($\hat{N}_n$, precursor ≈ 800, $\hat{N}_n \approx 140$) chain length PDMS, respectively. K3 is one of the SCALS with lowest CAH with water, and is grafted with intermediate chain length PDMS ($\hat{N}_n$, precursor ≈ 125, $\hat{N}_n \approx 65$).

The experimental FCS autocorrelation curves are shown with symbols on Figure 7a. The curves cannot be fitted with single component free Brownian diffusion model, typical of dye diffusion in bulk PDMS.[44] Instead, a more complex behavior was observed that can be best fitted with an anomalous 2D diffusion model:[45]

$$G(\tau) = \frac{1}{N} \times \frac{1}{1 + (\frac{\tau}{\tau_D})^{\alpha}} \quad (4)$$

where N is the average number of fluorescent tracers in the observation volume, τ_D is the diffusion time and α is the anomaly parameter. Fixing α to 0.7 (average value of the fits for the 3 curves) to enable a fit with only one parameter, the best fits yield the values of diffusion time τ_D shown in Figure 7b. These values show that the diffusion time τ_D of the tracers within layer K3 was the shortest of the three samples, while the longest τ_D was observed in layer K1 made from the short chain PDMS. Diffusion time is a proxy for the rate of molecular diffusion within the layer. The fact that the diffusion rate did not slow down continuously with the increase of the PDMS molecular weight is remarkable, as it contradicts expectations based on bulk diffusion[44] and

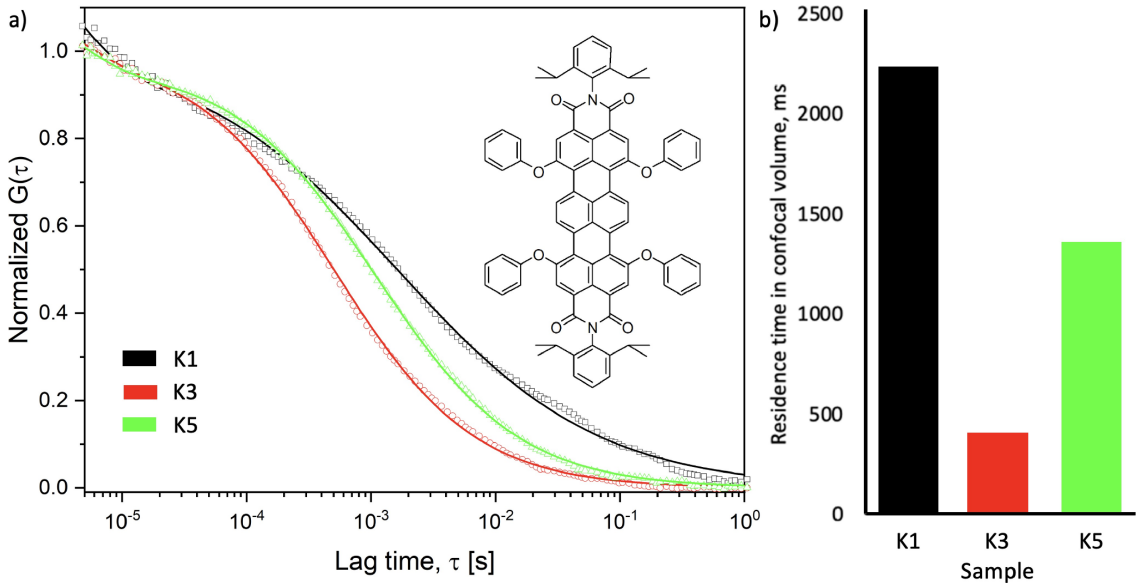

Figure 7. a) Normalized FCS autocorrelation function for TDI dye diffusing through PDMS SCALS corresponding to samples K1 ($\Sigma \approx 1.2$, $\hat{N}_n \approx 8$, CAH ≈ 12°), K3 ($\Sigma \approx 3$, $\hat{N}_n \approx 80$, CAH ≈ 5°), and K5 ($\Sigma \approx 4$, $\hat{N}_n = 140$, CAH = 14°) prepared according to the Krumpfer method;[3] b) The average residence time within the confocal volume extracted from fitting an anomalous diffusion model ($\alpha = 0.7$).

matches exactly the observed trends in CAH. The fact that the microviscosity within SCALS layers correlates with their CAH is strong evidence for the 'mobility hypothesis' that attributes the SCALS phenomenon to 'liquid-like mobility'.[4] The results here indicate that FCS is a promising technique for the study of the SCALS phenomenon. Future studies will use it to examine the correlation between grafting density, molecular weight and microviscosity.

Conclusions

The properties underpinning the ultra-low droplet adhesion of nano-thin PDMS grafted layers were investigated, and details of the reaction mechanism behind the most common method of SCALS preparation were revealed. The SCALS with the lowest measured CAH (1.5°) were those obtained with the method of Zhang et al.,[13] but the value of layer thickness was much lower than that reported by the authors (4 vs. 30 nm). In the synthetic method of Krumpfer and McCarthy,[3] chains with relatively low number of repeat units (<250) were confirmed to break on average once at their midpoint, as shown in the reaction scheme in Figure 1a. Longer chains instead break in multiple points during grafting, resulting in a nonlinear relationship between the molecular weight of the precursor and grafted chains and increasing the polydispersity of high molecular weight grafted chains. Including CO_2 snow-jet cleaning in the preparation steps leads to SCALS with lower CAH for most synthetic methods, despite leading to the detachment of a portion of the grafted chains for the longest chains studied (100–1000 repeat units), as revealed by the significant decrease in layer thickness.

Values of grafting density and chain length for SCALS were quantified, but did not correlate directly with values of CAH. Instead, the water CAH of SCALS was found to be satisfactorily predicted by their reduced grafting density, Σ. The lowest value of water CAH was achieved with PDMS chains in a brush regime, with $\Sigma = 2.5$, i.e. chains of about 40 repeat units (≈ 3 kDa), with layer thickness ≈ 3.5 nm and a grafting density of $\approx 0.75\ nm^{-2}$. At this reduced grafting density, the molecular mobility within the layer is at a maximum, as revealed by the residence time of a dye molecule within the grafted layers. The trends observed in molecular diffusion match those of CAH, suggesting a strong correlation of these properties. Combining the results from the novel application of three powerful surface-sensitive techniques, our study found that the exceptional low adhesion properties of SCALS are due to an ideal combination of layer uniformity and layer mobility: the PDMS chains must be sufficiently long and densely packed to uniformly coat the silicon wafers substrates, but not so tightly packed that chain entanglement compromises mobility. These results enable the rational design of SCALS and are an important step towards fully understanding their behavior. Chain configuration (dangling ends vs. loops) and polydispersity are important secondary factors that warrant further investigation.

Acknowledgements

We thank Prof. Frans Leermakers and Prof. Wiebe de Vos for valuable discussions regarding the implementation and interpretation of numerical self-consistent field theory. The authors acknowledge funding from the Australian Research Council (FT180100214), AINSE Ltd. (ECRG), and ANSTO for the provision of beamtime (P14012). SGL thanks AINSE Ltd. for providing financial assistance for the period when this work was completed (Honours Scholarship). Open Access publishing facilitated by The University of Sydney, as part of the Wiley - The University of Sydney agreement via the Council of Australian University Librarians.

Conflict of Interest

The authors declare no conflict of interest.

Data Availability Statement

The data that support the findings of this study are openly available in Zenodo at 10.5281/zenodo. 7992858doi], reference number 7992858.

Keywords: slippery surfaces · droplet mobility · self-assembled monolayers · polymer brush · single-molecule force spectroscopy

[1] L. R. Scarratt, U. Steiner, C. Neto, *Adv. Colloid Interface Sci.* **2017**, *246*, 133.
[2] S. Peppou-Chapman, J. K. Hong, A. Waterhouse, C. Neto, *Chem. Soc. Rev.* **2020**, *49* (11), 3688.
[3] J. W. Krumpfer, T. J. McCarthy, *Langmuir* **2011**, *27* (18), 11514.
[4] I. J. Gresham, C. Neto, *Adv. Colloid Interface Sci.* **2023**, *315*, 102906.
[5] J. O. Zoppe, N. C. Ataman, P. Mocny, J. Wang, J. Moraes, H.-A. Klok, *Chem. Rev.* **2017**, *117* (3), 1105.
[6] W. L. Chen, R. Cordero, H. Tran, C. K. Ober, *Macromolecules* **2017**, *50* (11), 4089.
[7] L. Chen, S. Huang, R. H. A. Ras, X. Tian, *Nat. Chem. Rev.* **2023**, *7* (2), 123.
[8] S. Wooh, D. Vollmer, *Angew. Chem.* **2016**, *55* (24), 6822.
[9] H.-J. Butt, J. Liu, K. Koynov, B. Straub, C. Hinduja, I. Roismann, R. Berger, X. Li, D. Vollmer, W. Steffen, M. Kappl, *Curr. Opin. Colloid Interface Sci.* **2022**, 101574.
[10] X. Zhao, B. Khatir, K. Mirshahidi, K. Yu, J. N. Kizhakkedathu, K. Golovin, *ACS Nano* **2021**, *15* (8), 13559.
[11] H. Teisala, P. Baumli, S. A. L. Weber, D. Vollmer, H.-J. Butt, *Langmuir* **2020**, *36* (16), 4416.
[12] L. Wang, T. J. McCarthy, *Angew. Chem.* **2016**, *55* (1), 244.
[13] L. Zhang, Z. Guo, J. Sarma, X. Dai, *ACS Appl. Mater. Interfaces* **2020**, *12* (17), 20084.
[14] K. Golovin, Design and application of surfaces with tunable adhesion to liquids and solids, **2017**, PhD Thesis, Chapter 5.
[15] D. H. Flagg, T. J. McCarthy, *Langmuir* **2017**, *33* (33), 8129.
[16] D. F. Cheng, C. Urata, B. Masheder, A. Hozumi, *J. Am. Chem. Soc.* **2012**, *134* (24), 10191.

[17] D. F. Cheng, C. Urata, M. Yagihashi, A. Hozumi, *Angew. Chem.* **2012**, *51* (12), 2956.
[18] W. J. Brittain, S. Minko, *J. Polym. Sci. Part A* **2007**, *45* (16), 3505.
[19] I. J. Gresham, T. J. Murdoch, E. C. Johnson, H. Robertson, G. B. Webber, E. J. Wanless, S. W. Prescott, A. R. J. Nelson, *J. Appl. Crystallogr.* **2021**, *54* (3), 739.
[20] G. Graffius, F. Bernardoni, A. Y. Fadeev, *Langmuir* **2014**, *30* (49), 14797.
[21] J. Sarma, L. Zhang, Z. Guo, X. Dai, *Chem. Eng. J.* **2022**, *431*, 133475.
[22] R. Lhermerout, K. Davitt, *Colloids Surf. A* **2019**, *566*, 148.
[23] S. Armstrong, G. McHale, R. Ledesma-Aguilar, G. G. Wells, *Langmuir* **2019**, *35* (8), 2989.
[24] H. Barrio-Zhang, É. Ruiz-Gutiérrez, S. Armstrong, G. McHale, G. G. Wells, R. Ledesma-Aguilar, *Langmuir* **2020**, *36* (49), 15094.
[25] R. Sherman, *Part. Sci. Technol.* **2007**, *25* (1), 37.
[26] D. Monga, Z. Guo, L. Shan, S. A. Taba, J. Sarma, X. Dai, *ACS Appl. Mater. Interfaces* **2022**, *14* (11), 13932.
[27] S. S. Sheiko, S. Panyukov, M. Rubinstein, *Macromolecules* **2011**, *44* (11), 4520–4529.
[28] N. C. Ataman, H. A. Klok, *Macromolecules* **2016**, *49* (23), 9035.
[29] I. J. Gresham, Archive of neutron reflectometry and AFM data, https://doi.org/10.5281/zenodo.7992858.
[30] T. Cosgrove, T. Heath, B. Van Lent, F. Leermakers, J. Scheutjens, *Macromolecules* **1987**, *20* (7), 1692.
[31] R. J. Sheridan, S. V. Orski, R. L. Jones, S. K. Satija, K. L. Beers, *Macromolecules* **2017**, *50* (17), 6668.
[32] W. M. de Vos, F. A. M. Leermakers, *Polymer* **2009**, *50* (1), 305.
[33] A. R. J. Nelson, A. McCluskey, I. J. Gresham, Refnx/refnx-models: User contributed models for refnx, https://github.com/refnx/refnx-models.
[34] T. J. Murdoch, B. A. Humphreys, J. D. Willott, K. P. Gregory, S. W. Prescott, A. Nelson, E. J. Wanless, G. B. Webber, *Macromolecules* **2016**, *49* (16), 6050.
[35] J. Ralston, I. Larson, M. W. Rutland, A. A. Feiler, M. Kleijn, *Pure Appl. Chem.* **2005**, *77* (12), 2149.
[36] I. J. Gresham, S. G. Lilley, AFM tools: A toolbox to manipulate AFM images and force curves in python, https://github.com/igresh/AFMtools.
[37] Y. Chen, X. Yu, L. Chen, S. Liu, X. Xu, S. Zhao, S. Huang, X. Tian, *Environ. Sci. Technol.* **2021**, *55* (13), 8839.
[38] M. Kruteva, *Adsorption* **2021**, *27* (5), 875.
[39] P. R. Dvornic, J. D. Jovanovic, M. N. Govedarica, *J. Appl. Polym. Sci.* **1993**, *49* (9), 1497.
[40] R. S. Hoy, G. S. Grest, *Macromolecules* **2007**, *40* (23), 8389.
[41] H. Vahabi, S. Vallabhuneni, M. Hedayati, W. Wang, D. Krapf, M. J. Kipper, N. Miljkovic, A. K. Kota, *Matter* **2022**, *5* (12), 4502.
[42] A. Katselas, I. J. Gresham, A. R. J. Nelson, C. Neto, *J. Chem. Phys.* **2023**, *158* (21), 214708.
[43] K. Koynov, H.-J. Butt, *Curr. Opin. Colloid Interface Sci.* **2012**, *17* (6), 377.
[44] T. Cherdhirankorn, V. Harmandaris, A. Juhari, P. Voudouris, G. Fytas, K. Kremer, K. Koynov, *Macromolecules* **2009**, *42* (13), 4858.
[45] P. Schwille, J. Korlach, W. W. Webb, *Cytometry* **1999**, *36* (3), 176.

Manuscript received: June 7, 2023
Accepted manuscript online: August 7, 2023
Version of record online: September 4, 2023